

# General solutions for nonlinear differential equations: a deep reinforcement learning approach

Shiyin Wei<sup>1,2,3,\*</sup>, Xiaowei Jin<sup>1,2,3,\*</sup>, Hui Li<sup>1,2,3,†</sup>

<sup>1</sup>*Key Lab of Smart Prevention and Mitigation of Civil Engineering Disasters of the Ministry of Industry and Information Technology, Harbin Institute of Technology, Harbin 150090, China*

<sup>2</sup>*Key Lab of Structures Dynamic Behavior and Control of the Ministry of Education, Harbin Institute of Technology, Harbin 150090, China*

<sup>3</sup>*School of Civil Engineering, Harbin Institute of Technology, Harbin 150090, China*

## Abstracts

Physicists use differential equations to describe the physical dynamical world, and the solutions of these equations constitute our understanding of the world. During the hundreds of years, scientists developed several ways to solve these equations, i.e., the analytical solutions and the numerical solutions. However, for some complex equations, there may be no analytical solutions, and the numerical solutions may encounter the curse of the extreme computational cost if the accuracy is the first consideration. Solving equations is a high-level human intelligence work and a crucial step towards general artificial intelligence (AI), where deep reinforcement learning (DRL) may contribute. This work makes the first attempt of applying (DRL) to solve nonlinear differential equations both in discretized and continuous format with the governing equations (physical laws) embedded in the DRL network, including ordinary differential equations (ODEs) and partial differential equations (PDEs). The DRL network consists of an actor that outputs solution approximations policy and a critic that outputs the critic of the actor's output solution. Deterministic policy network is employed as the actor, and governing equations are embedded in the critic. The effectiveness of the DRL solver in Schrödinger equation, Navier-Stocks, Van der Pol equation, Burgers' equation and the equation of motion are discussed.

---

\* These authors contributed to the work equally and should be regarded as co-first authors.

† Corresponding author. E-mail address: lihui@hit.edu.cn.

## Introduction

Differential equations, including ordinary differential equations (ODEs) and partial differential equations (PDEs), formalize the description of the dynamical nature of the world around us. However, solving these equations is a challenge due to extreme computational cost, although limited cases have analytical or numerical solutions<sup>1-3</sup>.

Solving equations is a high-level human intelligence work and a crucial step towards general artificial intelligence. Therefore, the obstacle of extreme computational cost in numerical solution may be bypassed by using general AI techniques, such as deep learning and reinforcement learning<sup>4, 5</sup>, which are rapidly developed during the last decades. Recent years such efforts have been made, and three main kinds of the existed efforts using deep learning can be categorized into: 1) directly map to the solution represented by the deep neural network in the continuous manner as in the analytical solution<sup>6</sup>, data used to train the network is randomly sampled within the entire solution domain in each training batch, including initial conditions and boundary conditions; 2) directly map to the solution in the discretized manner as in the numerical solution<sup>7-9</sup>; and 3) indirectly map to the internal results or parameters of the numerical solutions, and use the internal results to derive the numerical solutions<sup>6, 10</sup>.

The essence is to take advantage of the nonlinear representing ability of deep neural networks. The solutions are either directly output by the network or numerically derived from the outputs of the neural network, and the solution task is regarded as a weak-label task while the governing equation is treated as the weak-label to calculate the loss function of the network. The term ‘weak-label’ is emphasized to make difference with the label in supervised learning, i.e., the true solutions are not known in these tasks, however, when we get a candidate solution by the neural network output, we can tell how far the output solution is to the true solution by the imbalance of the physical law.

Because of the weak-label property, the solution using deep learning may be unstable for high-dimensional ODEs/PDEs tasks. Hence, we propose a deep reinforcement learning (DRL) paradigm for the ODEs/PDEs solution. DRL is naturally suitable for weak-label tasks by the trial-error learning mechanism<sup>5, 11</sup>. Take the game of Go for example<sup>12</sup>, the only prior information about the task is the playing rules that defines win or lose, the label (or score) of each step is whether win or lose after the whole episode of playing rather than an exact score.

While employing reinforcement learning, we are essentially treating the solving of differential equations as a control task. The state is the known current-step solution (either the given initial condition or the intermediate DRL solution) of the differential equations, the action is the solution of the task, and the goal is to find a proper action to balance the governing equation with an acceptable error. A deep deterministic policy network is used to output action policy given a state, and the governing equation is used as the critic, gradients of the policy network is calculated based on the critic.

## Results

### Nonlinear differential equations

A general nonlinear differential equation form is written as:

$$u_t + \mathcal{N}(u, \lambda) = 0 \quad (1)$$

where  $u(x, t)$  denotes the state, and in the solution task, it is also the latent solution of the equation;

$u_t$  is the derivative with respect to time;  $\mathcal{N}(\cdot, \lambda)$  is a nonlinear operator parameterized by  $\lambda$ .

Following lists some well-known ODEs and PDEs in the general form that used as examples in this paper.

#### (1) Van der Pol equation

Van der Pol equation is an oscillator with nonlinear damping governed by the second-order differential equation<sup>13</sup>

$$u_{tt} - \alpha(1 - u^2)u_t + u = \beta p(t) \quad (2)$$

where  $u_{tt}$  is the second-order derivative,  $\alpha, \beta > 0$  are the scalar parameter, and  $p(t)$  is the external excitation. High-order differential equations can always be rewritten in the state representation form to be consistent with Eq. (1) like

$$\begin{aligned} x_t &= y \\ y_t &= \alpha(1 - x^2)y - x + \beta p(t) \end{aligned} \quad (3)$$

Therefore, in the following of this paper, we use their most well-known high-order form.

#### (2) Equation of motion

Equation of motion is frequently used to describe the structural or system dynamics<sup>14</sup>, the

nonlinear form with Bouc-Wen hysteresis model for single degree of freedom (SDOF) system and multi-degree of freedom (MDOF) system illustrated in Fig. 1 are written as,

$$\begin{aligned} mu_{\dot{t}} + cu_{\dot{t}} + \alpha ku + (1-\alpha)kz &= p(t) \\ z_{\dot{t}} &= Au - \beta z |u_{\dot{t}}| |z|^{n-1} - \gamma u_{\dot{t}} |z|^n \end{aligned} \quad (4)$$

$$\begin{aligned} MU_{\dot{t}} + CU_{\dot{t}} + \alpha K_1 U + (1-\alpha)K_2 Z &= P(t) \\ U &= (u_1, u_2, \dots, u_N) \quad Z = (z_1, z_2, \dots, z_N) \\ z_{\dot{t}j} &= Ay_{\dot{t}j} - \beta z_j |y_{\dot{t}j}| |z_j|^{n-1} - \gamma y_{\dot{t}j} |z_j|^n \quad (j=1, 2, \dots, N) \\ y_1 &= u_1 \quad y_j = u_j - u_{j-1} \quad (j=2, 3, \dots, N) \end{aligned} \quad (5)$$

where  $m, c, k$  ( $M, C, K$ ) represent the mass, damping, and stiffness (matrix) of the structure in SDOF (MDOF) system respectively,  $p(t)$  ( $P(t)$ ) is the external excitation,  $\alpha ku, (1-\alpha)kz$  ( $\alpha K_1 U, (1-\alpha)K_2 Z$ , where  $K_1, K_2$  are the linear and nonlinear stiffness matrix) are the linear and nonlinear resilience respectively,  $A, \beta, \gamma, n$  are Bouc-Wen parameters that control the shape and size behavior of the hysteresis model,  $y_j, z_j$  are the interlayers displacement and resilience, and  $y_{\dot{t}j}, z_{\dot{t}j}$  are the derivative of  $y_j$  and  $z_j$ .

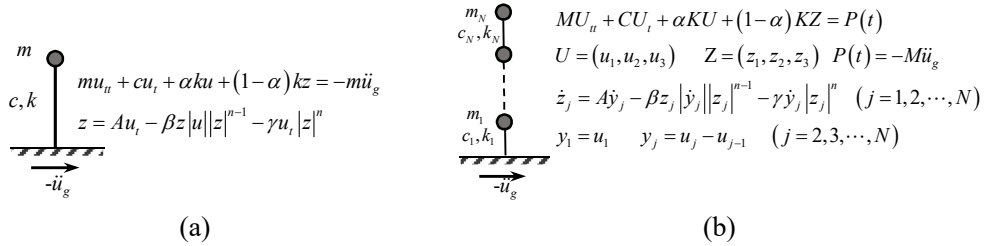


**Fig. 1** Equation of motion equation under earthquake signal: (a) SDOF; and (b) MDOF.

### (3) Burgers equation

Burgers equation are common in various domains, such as nonlinear acoustics and gas dynamics, etc<sup>15</sup>. The general form of the Burgers equation is,

$$\frac{\partial \mathbf{u}}{\partial t} + (\mathbf{u} \cdot \nabla) \mathbf{u} - \nu \nabla^2 \mathbf{u} = 0 \quad (6)$$

where  $\mathbf{u}(\mathbf{x}, t)$  is a given field and  $\nu$  is the diffusion coefficient.

#### (4) Schrödinger equation

The Schrödinger equation describes the changes of the quantum state of a physical system over time<sup>16</sup>, and the nonlinear Schrödinger equation involved in this study is,

$$\frac{\partial u}{\partial t} = 0.5i \frac{\partial^2 u}{\partial x^2} + i|u|^2 u \quad (7)$$

#### (5) Navier-Stocks equations

For a Newtonian incompressible fluid, the governing Navier-Stocks (N-S) equations are,

$$\begin{aligned} \frac{\partial \mathbf{u}}{\partial t} + (\mathbf{u} \cdot \nabla) \mathbf{u} &= -\frac{1}{\rho} \nabla p + \frac{\mu}{\rho} \nabla^2 \mathbf{u}, \\ \nabla \cdot \mathbf{u} &= 0 \end{aligned} \quad (8)$$

where  $\mathbf{u}(\mathbf{x}, t)$  is the velocity field,  $p(\mathbf{x}, t)$  is the pressure,  $\rho$  is the density of the fluid and  $\mu$  is the viscosity coefficient.

### Deep reinforcement learning framework

Deep neural networks have shown remarkable success in the learning of high-dimensional nonlinear functions<sup>17, 18</sup>, although without a solid theoretical framework for understanding what is inside the black box. Given the necessary condition for solving the differential equations, i.e., the initial condition and boundary condition (which is also the solution of the equations in initial and boundary state), the solution of the equation is a nonlinear mapping from the initial and boundary solutions to the temporal-spatial field solutions. This enables the deep neural network approximator parameterized by  $\theta$  to represent the solution of the differential equations.

The intuitive of employing DRL to solve differential equations is that the process of solving equations can be dealt as a trial-error process, the process contains two periods: first guess a candidate solution  $a \in \mathcal{A}$  under the given state  $s \in \mathcal{S}$ ; then criticize and improve it by calculating the loss function using the governing equation, where  $\mathcal{A}$  and  $\mathcal{S}$  are the continuous domain of the solution, therefor  $\mathcal{A} = \mathcal{S}$ .

As illustrated in Fig. 2, in DRL, a deep neural network approximator is employed as the implementation of action choice, also termed as the policy network  $\pi_\theta(s_t, a_t) = P(a_t | s_t, \theta)$  that

takes the current known state  $s_t$  of equation (or current step solution) as the input and outputs the candidate solution action  $a_t$  by the parameterized probability  $P$ : for the continuous form, the input state  $s_t$  are the function of the temporal and spatial location  $x, t$  and the initial and boundary solution, the output action  $a_t$  is the continuous solution  $\hat{u}(x, t)$ ; for the temporal discretized form, the input state  $s_t$  are the temporal and spatial location and the current step solution (for initial step, it is the initial solution; for other steps, it is the DRL predicted solution), and the output action  $a_t$  is the next step solution  $\hat{u}(x, t+1)$ . The imbalance of the governing equation  $r = -(\hat{u} - \mathcal{N}(\hat{u}, \lambda))^2$  is taken as the critic, and the goal of the solving task is to find a proper policy that makes  $r$  within the error threshold.

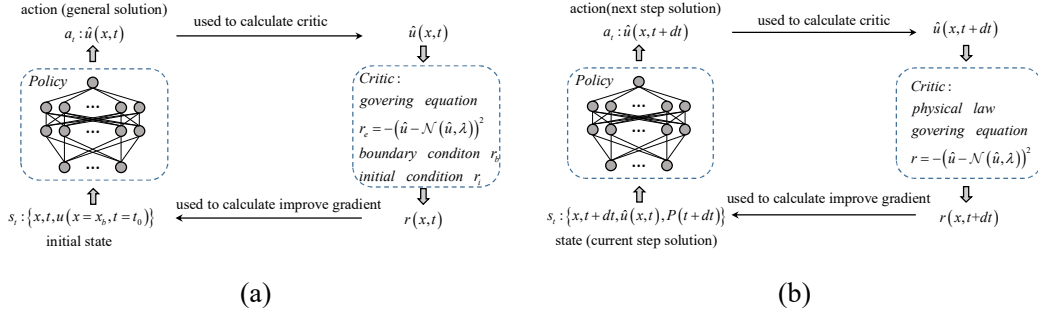


**Fig. 2** The DRL framework for equation solution: (a) continuous form; and (b) temporal discretized form.

As the governing equation is the prior knowledge, the solving task can be handled as a one-step Markov Decision Process (MDP) task. The loss function of the policy network over the continuous solution action space is written as (for convenience, symbols used are from the classic reinforcement learning; however, one can correspond to the specific solution problem according to the diagram in Fig. 2):

$$J(\theta) = \mathbb{E}_{\pi_{\theta}} [r] = \int_{\mathcal{A}} \pi_{\theta}(s, a) r(s, a) da \quad (9)$$

Silver et.al shows an outperformed power of the deterministic version of the policy gradient (DPG) that requires less sample to train<sup>19</sup>, i.e., parameterize the policy by a deterministic policy  $\mu_{\theta} : \mathcal{S} \rightarrow \mathcal{A}$  and a variance  $\sigma$ . The policy gradient is as follows,

$$\nabla_{\theta} J(\theta) = \int_{\mathcal{A}} \nabla_{\theta} \pi_{\theta}(s, a) r(s, a) da = \int_{\mathcal{A}} \nabla_{\theta} \mu_{\theta}(s) r(s, \mu_{\theta}(s)) da \quad (10)$$

In a Monte-Carlo sampling perspective, Eq. (10) is rewritten as

$$\nabla_{\theta} J(\theta) \approx \frac{1}{N} \sum_i \nabla_{\theta} \mu_{\theta}(s) r(s, \mu_{\theta}(s)) \quad (11)$$

where  $N$  is the sampled batch size in training, and the variance  $\sigma$  is a decayed scalar during the training process.

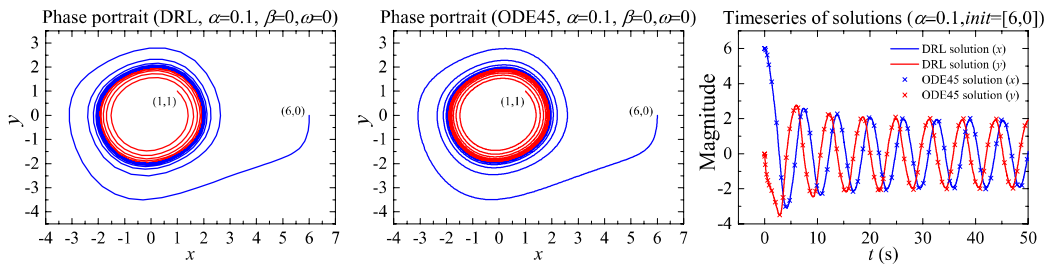
## Example Simulations

### (1) Temporal discretized DRL

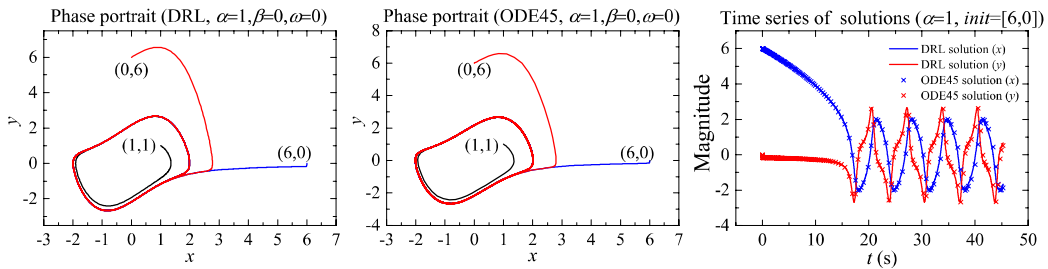
**Van der Pol equations.** In the learning of Van der Pol equation, the input of the policy network is the current-step solution of the Van der Pol system  $\{x(t_i), y(t_i)\}$  in Eq. (3), temporal interval  $dt$  is set as 0.001s; the derivative of time is set as the ruler forward difference; the critic derives as Eq. (12) and the error threshold is set as 1E-4,

$$r(t+dt) = - \left( \frac{\hat{x}(t+dt) - x(t)}{dt} - \hat{x}_i(t+1) \right)^2 - \left( \frac{\hat{y}(t+dt) - y(t)}{dt} - \alpha(1 - \hat{x}(t+dt)^2) + \hat{x}(t+dt) - \beta p(t+dt) \right)^2, \quad (12)$$

Figure 3 illustrates the results compared with the ODE45 method (the explicit Runge-Kutta (4, 5) method), and results agree well with each other<sup>20</sup>. It shows that the DRL approach is effective in solving Van der Pol equations.



(a)



(b)

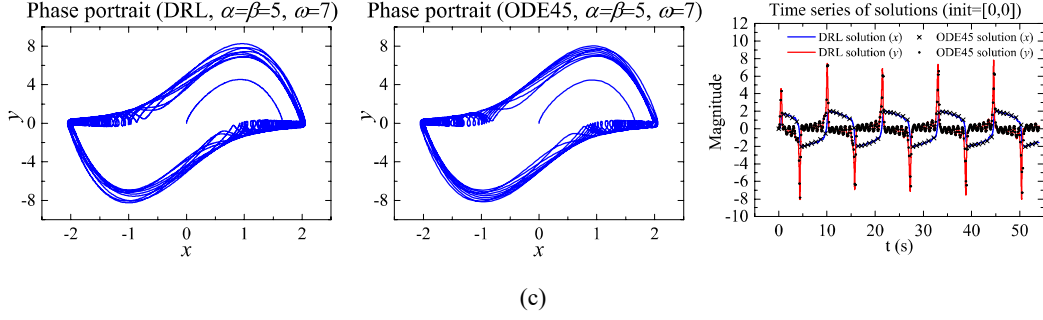


**Fig. 3** Comparison between DRL and others: (a) unforced system  $\alpha = 0.1$ ; (b) unforced system  $\alpha = 1$ ; (c) forced system  $\alpha = \beta = 5, \omega = 7$ .

**Equation of motion.** Take the three-degree of freedom system as an example, the structural parameters are

$$\begin{aligned}
 M &= \begin{pmatrix} m_1 & & \\ & m_2 & \\ & & m_3 \end{pmatrix} \quad C = \begin{pmatrix} c_1 + c_2 & -c_2 & \\ -c_2 & c_2 + c_3 & -c_3 \\ & -c_3 & c_3 \end{pmatrix} \\
 K_1 &= \begin{pmatrix} k_1 + k_2 & -k_2 & \\ -k_2 & k_2 + k_3 & -k_3 \\ & -k_3 & k_3 \end{pmatrix} \quad K_2 = \begin{pmatrix} k_1 & -k_2 & \\ & k_2 & -k_3 \\ & & k_3 \end{pmatrix} \\
 m_1 = m_2 = m_3 &= 1\text{kg} \quad c_1 = c_2 = c_3 = 2\text{N} \cdot \text{s} / \text{m} \quad k_1 = k_2 = k_3 = 100\text{N} / \text{m} \\
 P(t) &= -M(\ddot{u}_g, \ddot{u}_g, \ddot{u}_g)^T \\
 \alpha &= 0.1, A = 1, \beta = 0.5, \gamma = 0.05, n = 1
 \end{aligned}$$

where  $\ddot{u}_g$  is the external earthquake excitation, and is chosen as the El Centro signal. The inputs of the policy network is set as  $\{U(t), U_i(t), U_u(t), Z(t), P(t+dt)\}$  and the output is set as  $U(t+dt)$ , while  $Z(t+dt), Z_i(t+dt)$  are updated according to the Bouc-Wen model and Euler forward difference method, and  $U_i(t+dt), U_u(t+dt)$  are updated according to the numerical method in<sup>14</sup>,

$$\begin{aligned}
 dU(t) &= dtU_i(t) + \frac{(dt)^2}{2}U_u(t) + \frac{(dt)^2}{6}dU_u(t), \\
 dU_i(t) &= dtU_u(t) + \frac{dt}{2}dU_u(t), \\
 U_u(t+dt) &= U_u(t) + dU_u(t), \quad U_i(t+dt) = U_i(t) + dU_i(t)
 \end{aligned}$$

Temporal interval is set as 0.01s, and the threshold of critic is set as 1E-3. Fig. 4 illustrates the solution result.



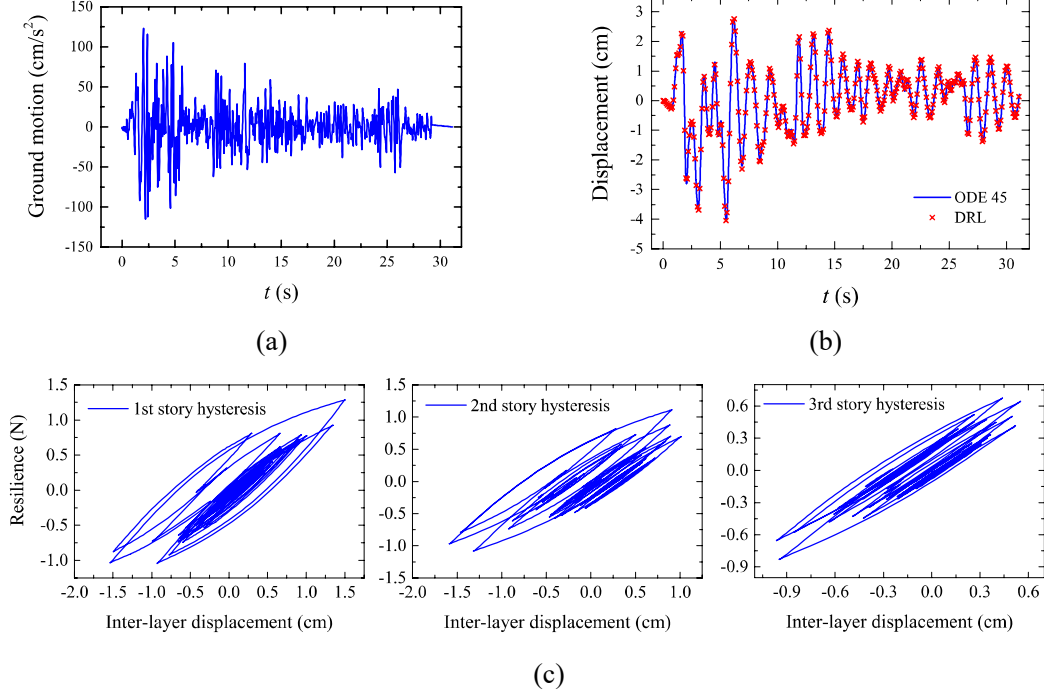


**Fig. 4** Three--DOF structure motion equation solution: (a) El Centro earthquake as the external excitation (b) the displacement response of the 3rd story; (c) the DRL nonlinear hysteresis of the MDOF

## (2) Temporal continuous DRL

**Burgers' equation.** For PDEs, the inputs of the policy network will become cumbersome when the equation is discretized in spatial and temporal dimensions. Instead, the policy network in the deep reinforcement learning framework is written as,

$$\hat{\mathbf{u}}(\mathbf{x}, t) = f(\mathbf{x}, t | \theta) \quad (13)$$

where  $\theta$  is the trainable variable in the policy network. A deep neural network consisting of seven hidden layers is used for inferring the policy. The number of nodes in each hidden layer is [20 30 40 40 40 30 20], and the activation function is tanh. Then all terms in the Burgers' equation can be derived as,

$$\frac{\partial \mathbf{u}}{\partial t} = \frac{\partial f}{\partial t}, \quad \frac{\partial \mathbf{u}}{\partial x} = \frac{\partial f}{\partial x}, \quad \frac{\partial^2 \mathbf{u}}{\partial x^2} = \frac{\partial^2 f}{\partial x^2}$$

The critic for this equation is,

$$\begin{aligned} r &= \lambda r_b + \mu r_i + r_e, \\ r_b &= MSE_b = -\frac{1}{N_b} \sum (\hat{\mathbf{u}}(\mathbf{x}_b, t) - \mathbf{u}(\mathbf{x}_b, t))^2, \\ r_i &= MSE_i = -\frac{1}{N_i} \sum (\hat{\mathbf{u}}(\mathbf{x}_i, 0) - \mathbf{u}(\mathbf{x}_i, 0))^2, \end{aligned} \quad (14)$$

$$r_e = MSE_e = -\frac{1}{N_e} \sum \left( \frac{\partial \hat{\mathbf{u}}}{\partial t} - (\hat{\mathbf{u}} \cdot \nabla) \hat{\mathbf{u}} - \alpha \nabla^2 \hat{\mathbf{u}} \right)^2$$

where  $N_b$ ,  $N_i$ ,  $N_e$  are sampled points for boundary condition, initial condition and the equation, respectively;  $\lambda$  and  $\mu$  are hyperparameters preventing the effects of imbalanced sampling. Then, the loss function is,

$$J(\theta) = E_{\pi_\theta} [r] = \int_S \int_A \pi_\theta(s, a) r(s, a) da \quad (15)$$

The diffusion coefficient is a critical parameter which influences the solution topology of the Burgers' equation, and three diffusion coefficients are considered in this study. Take one-dimensional Burger's equations as an example, the diffusion coefficient, the computational domain, the initial and boundary conditions are set as follows,

$$\nu = 0.1, 0.05 \text{ and } 0.01, \quad x \in [-1, 1], \quad t \in [0, 1],$$

$$u(x, 0) = -\sin(\pi x),$$

$$u(-1, t) = u(1, t) = 0$$

The number of spatial-temporal points sampled in this example are  $N_b = 50$ ,  $N_i = 50$  and  $N_e = 10,000$ , respectively. The learning rate is set to exponential decay, with an initial value of 0.005 and decay rate 0.9995 (decaying every 100 steps, but no less than 1E-5). It should be noted that the solutions of this PDE is governed by its boundary conditions and initial conditions. Hence,  $\lambda$  and  $\mu$  are set large values at the beginning to accelerate the training process, the exponential decay is applied to these two parameters, with an initial value of 50 and decay rate 0.9 (decaying every 100 steps, but no less than 2).

After iterations the mean square error  $r_b + r_i + r_e$  converges to less than 6E-5 for all the diffusion coefficients cases. The comparisons between the DRL solutions and the solutions derived by Cole<sup>1</sup> are shown in Fig. 5. The DRL solutions, i.e., the spatial-temporal cloud map of the solution and the solutions selected at some spatial and temporal points, agree well with Cole's results. As shown in Fig. 5d, shock wave appears as the decrease of  $\nu$ , and the absolute value of the first derivative is quite large. However, the DRL solutions can accurately capture the shock wave.

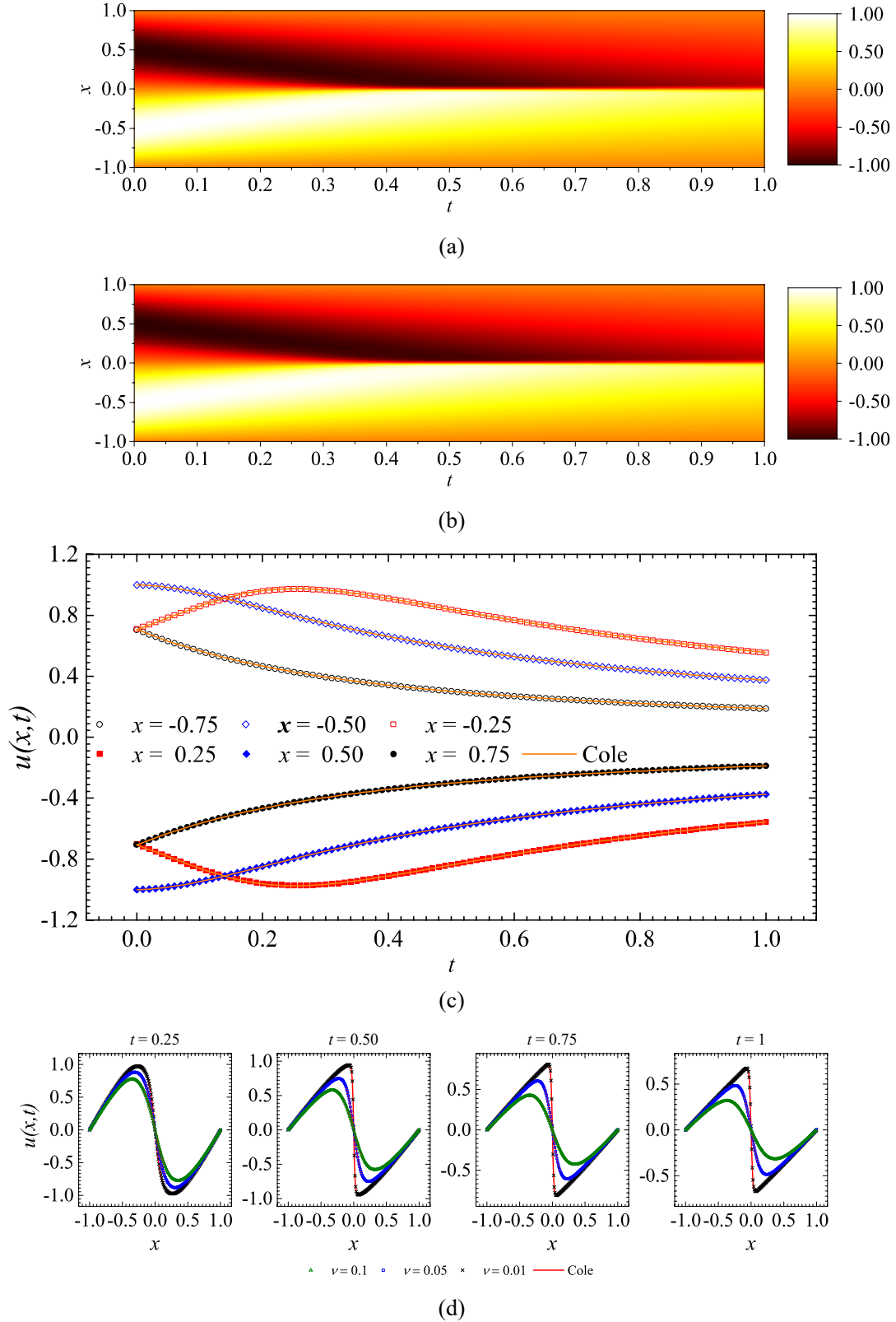


**Fig. 5** One-dimensional Burgers' equation solution: (a) spatial-temporal solution of Cole for  $\nu = 0.01$ ; (b) spatial-temporal DRL solution for  $\nu = 0.01$ ; (c) comparison between the DRL solution and exact solution at six selected spatial points for  $\nu = 0.01$ ; (d) comparison between the DRL solution and exact solution at four selected temporal snapshots for various diffusion coefficients.

**Schrödinger equation.** The computational domain, the initial and boundary conditions of the Schrödinger equation are set as follows,

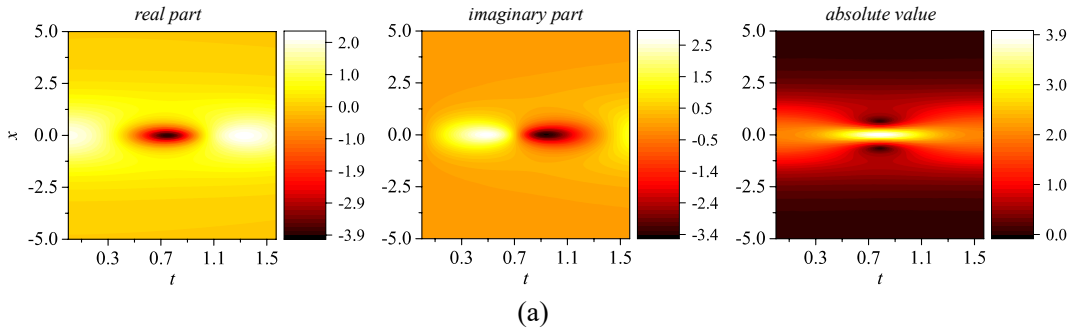
$$x \in [-5, 5], \quad t \in [0, \pi / 2],$$

$$u(x, 0) = 2 \operatorname{sech}(x),$$

$$u(t, -5) = u(t, 5),$$

$$\left. \frac{\partial u}{\partial x} \right|_{x=-5} = \left. \frac{\partial u}{\partial x} \right|_{x=5}$$

A deep neural network consisting of seven hidden is used for inferring the policy. The architecture of hidden layers is the same as that used for solving the Burgers' equation. The loss function is similar as Eqs. (14) and (15) according to the physical law and boundary/initial conditions. The learning rate is set to decaying from 0.005 to 3E-5. In addition,  $\lambda$  and  $\mu$  are set large values at the beginning to accelerate the training process, and they decay from 50 to 2. The number of spatial-temporal points sampled in this example are  $N_b = 50$ ,  $N_i = 50$  and  $N_e = 20,000$ , respectively. After iterations, the mean square error converges to less than 1.4E-4. Comparisons between the DRL solutions and the numerical solutions obtained by a high-order numerical method, i.e., the fourth-order Runge-Kutta exponential time differencing method (ETD4RK)<sup>21, 22</sup>, are shown in Fig. 6. Both real part and imaginary part of DRL solutions, i.e., the spatial-temporal cloud map of the solution and the solutions selected at some spatial points, agree well with ETD4RK solution.



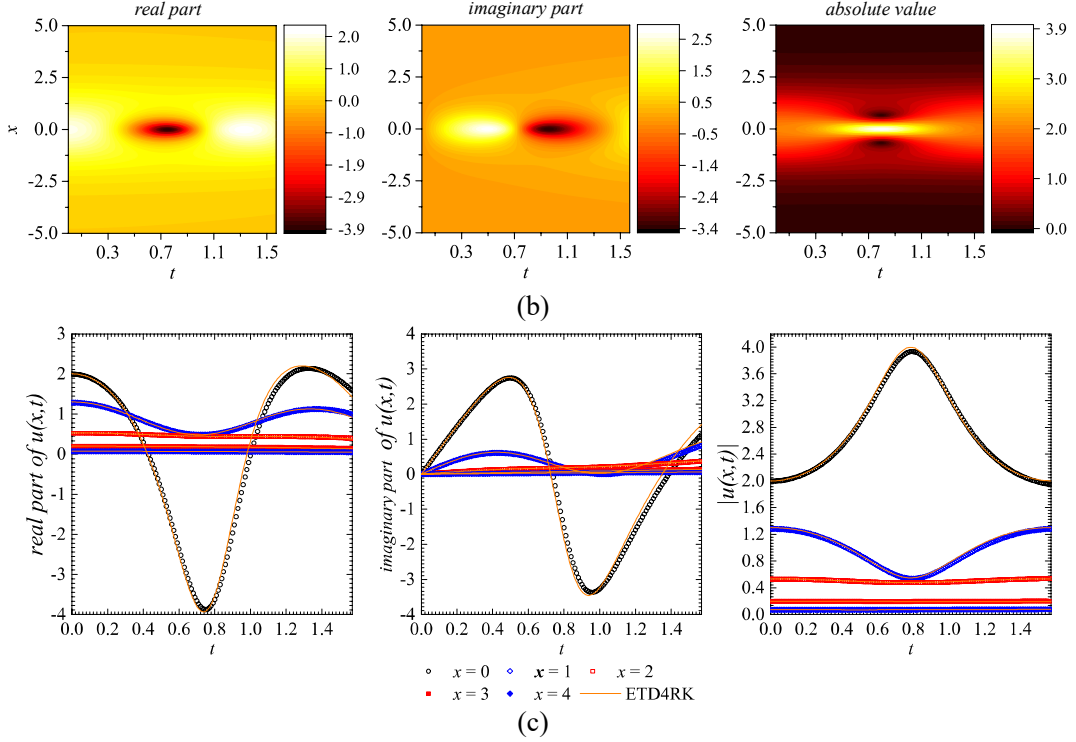


**Fig. 6** One-dimensional Schrodinger equation solution: (a) spatial-temporal ETD4RK solution; (b) spatial-temporal DRL solution; (c) comparison between the DRL solution and exact solution at five selected spatial points.

**Couette flow.** To test the possible application of DRL approach to fluid dynamics, the steady Couette flow in Fig. 7 is taken as an example. The governing equations are formulated as,

$$(\mathbf{u} \cdot \nabla) \mathbf{u} = -\frac{1}{\rho} \nabla p + \frac{\mu}{\rho} \nabla^2 \mathbf{u}$$

$$\nabla \cdot \mathbf{u} = 0$$

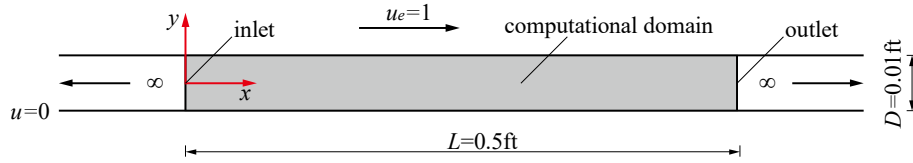


**Fig. 7** Computational domain of Couette flow.

The computational domain, the initial and boundary conditions of the N-S equation are set as follows,

$$x \in [0, 0.5], \quad y \in [-0.005, 0.005],$$

$$u = u_e = 1 \Big|_{y=0.005}, \quad v = 0 \Big|_{y=0.005}, \quad u = v = 0 \Big|_{y=-0.005},$$

$$p = 0 \Big|_{x=0}, \quad v = 0 \Big|_{x=0}, \quad p = 0 \Big|_{x=0.5}$$

Three policy networks are used in the deep reinforcement learning framework,

$$\begin{aligned}\hat{u}(x, y) &= f_u(x, y | \theta_u), \\ \hat{v}(x, y) &= f_v(x, y | \theta_v), \\ \hat{p}(x, y) &= f_p(x, y | \theta_p)\end{aligned}\tag{16}$$

where  $\theta_u$ ,  $\theta_v$  and  $\theta_p$  are trainable parameters of the three networks, respectively. The architecture of hidden layers for each policy network is the same as that used for solving the Burgers' equation. The number of spatial-temporal points sampled in this example are  $N_b = 4,000$ ,  $N_t = 2,000$  and  $N_e = 20,000$ , respectively. The learning rate is set to decaying from 0.001 to  $1.5E-6$ . Hyperparameters  $\lambda$  is set to 1 in this example. After iterations, the mean square error converges to less than  $1.58E-4$ . The DRL solution is shown in Fig. 8a. The deep reinforcement learning approach solves the correct velocity distribution of the Couette flow. Fig. 8b shows the convergence process of this method.

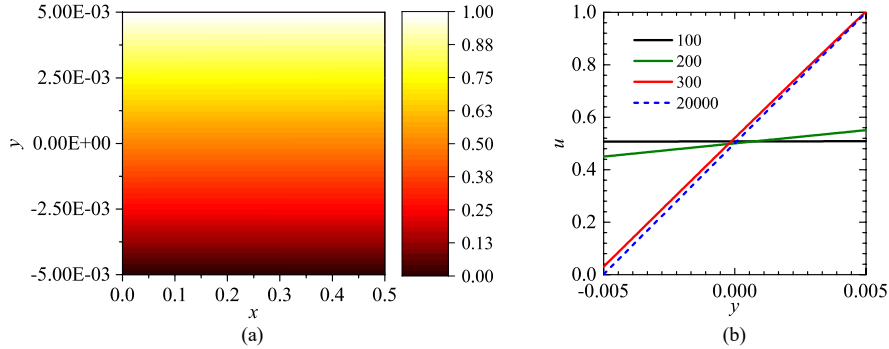


**Fig. 8** Couette flow solution: (a) spatial-temporal DRL solution; (b) streamwise velocity at  $x = 0.25$  for various iteration steps.

## Discussion

In summary, we presented a new perspective of the solving of differential equations as the control task that tries to balance the equation, hence proposed a deep reinforcement learning (DRL) paradigm for solving equations: the current-step solution is considered to be the state of the task, and the possible solution is considered as the action that we take in the task. In the DRL paradigm, a policy network, structured by a deep neural network with the continuous state as the input and the continuous action as the output, acts as the actor that outputs candidate solutions; and the physical governing equation acts as the critic that indicates the balance of the equation when substituting the candidate solution in the differential equation. Gradients of the policy network is calculated based

on the critic, and the deterministic policy gradient architecture is employed. Both continuous form and discretized form are demonstrated in the solving of PDEs and ODEs, respectively.

Specifically, the initial condition of the ODEs is handled as the initial state in the DRL approach, and the solving of the ODEs in discretized representation presents to be the one-step MDP problem that gives the current-step solution to output the next-step solution; governing equation presents as the critic. In the solving of PDEs in continuous form, the spatial-temporal coordinates and the current-step solution are treated as the state in DRL, and the solution is treated as the output of the policy network, while the governing equations, boundary conditions and initial conditions are used as the critic. All the DRL solutions of these differential equations agree well with the high-order numerical methods or analytical solutions. Especially, this study shows the potential of the DRL approach to solve the Navier-Stokes equations, although only a steady Couette flow case is tested. Future work may involve the development of the DRL approach to solve complex systems, such as chaos and turbulent flows.

## Methods

**Setting of DRL hyperparameters.** Adam (adaptive moment estimation)<sup>23</sup> is employed as the optimization algorithm for training the policy network, in which learning rate is an essential hyperparameter. Meanwhile, the selection of activation functions, the number of hidden layers, the number of nodes of each hidden layer in the deep policy network and the discretized time-step for the discretized form of DRL approach are also hyperparameters to be set. The decay rate of the deviation  $\sigma = 0.9995$  for every 100 training steps. The selection of these hyperparameters can be found above.

**Code availability.** Python and MATLAB codes for the examples appeared in this research are available from [https://github.com/HIT-SMC/DRL\\_solver](https://github.com/HIT-SMC/DRL_solver).

## Acknowledgement

This research was funded by the National Natural Sciences Foundation of China (NSFC) (Grant Nos. 51638007 and U1711265).

## Reference

1. Cole JD. On a quasi-linear parabolic equation occurring in aerodynamics. *Quarterly of applied mathematics* **9**, 225-236 (1951).

2. Soliman AA. The modified extended tanh-function method for solving Burgers-type equations. *Physica A: Statistical Mechanics and its Applications* **361**, 394-404 (2006).
3. Feit M, Fleck Jr J, Steiger A. Solution of the Schrödinger equation by a spectral method. *Journal of Computational Physics* **47**, 412-433 (1982).
4. LeCun Y, Bengio Y, Hinton G. Deep learning. *Nature* **521**, 436-444 (2015).
5. Sutton RS, Barto AG. *Introduction to reinforcement learning*. MIT press Cambridge (1998).
6. Raissi M, Perdikaris P, Karniadakis GE. Physics Informed Deep Learning (Part I): Data-driven Solutions of Nonlinear Partial Differential Equations. *arXiv preprint arXiv:171110561*, (2017).
7. Han J, Jentzen A. Overcoming the curse of dimensionality: Solving high-dimensional partial differential equations using deep learning. *arXiv preprint arXiv:170702568*, (2017).
8. Mills K, Spanner M, Tamblyn I. Deep learning and the Schrödinger equation. *Physical Review A* **96**, 042113 (2017).
9. E W, Han J, Jentzen A. Deep learning-based numerical methods for high-dimensional parabolic partial differential equations and backward stochastic differential equations. *Communications in Mathematics and Statistics* **5**, 349-380 (2017).
10. Khoo Y, Lu J, Ying L. Solving parametric PDE problems with artificial neural networks. *arXiv preprint arXiv:170703351*, (2017).
11. Mnih V, et al. Playing atari with deep reinforcement learning. *arXiv preprint arXiv:13125602*, (2013).
12. Silver D, et al. Mastering the game of Go with deep neural networks and tree search. *nature* **529**, 484-489 (2016).
13. Guckenheimer J, Holmes P. *Nonlinear oscillations, dynamical systems, and bifurcations of vector fields*. Springer Science & Business Media (2013).
14. Chopra AK. *Dynamics of structures: theory and applications to earthquake engineering* (2007).
15. Hopf E. The partial differential equation  $u_t + u u_x = \mu x x$ . *Communications on Pure and Applied mathematics* **3**, 201-230 (1950).
16. Schrödinger E. An undulatory theory of the mechanics of atoms and molecules. *Physical review* **28**, 1049 (1926).
17. Li S, Laima S, Li H. Data-driven modeling of vortex-induced vibration of a long-span suspension bridge using decision tree learning and support vector regression. *Journal of Wind Engineering and Industrial Aerodynamics* **172**, 196-211 (2018).
18. Jin X, Cheng P, Chen W-L, Li H. Prediction model of velocity field around circular cylinder over various Reynolds numbers by fusion convolutional neural networks based on pressure on the cylinder. *Physics of Fluids* **30**, 047105 (2018).
19. Silver D, Lever G, Heess N, Degris T, Wierstra D, Riedmiller M. Deterministic policy gradient algorithms. In: *ICML* (2014).
20. Tsatsos M. Theoretical and Numerical study of the Van der Pol equation. *Doctoral desertation, Aristotle University of Thessaloniki* **4**, 6 (2006).
21. Cox SM, Matthews PC. Exponential time differencing for stiff systems. *Journal of Computational Physics* **176**, 430-455 (2002).
22. Driscoll TA, Hale N, Trefethen LN. *Chebfun guide*. Pafnuty Publications, Oxford (2014).
23. Kingma DP, Ba J. Adam: A method for stochastic optimization. *arXiv preprint arXiv:14126980*, (2014).